UK Atomic Energy Authority

UKAEA-STEP-PR(21)02

J. Fradera, S. Sadaba, F. Calvo, S. Ha, S. Merriman,
P. Gordillo, J. Connell, A. Elfaraskoury, B. Echeveste

Encapsulated Fuel Breeder Blanket

Encapsulated Fuel Breeder Blanket

J. Fradera, S. Sadaba, F. Calvo, S. Ha, S. Merriman, P. Gordillo, J. Connell, A. Elfaraskoury, B. Echeveste

This is a preprint of a paper submitted for publication in
Nuclear Engineering and Design

Graphical Abstract

Encapsulated breeder commercial blanket conceptual design

J. Fradera, S. Sadaba, F. Calvo, S. Ha, S. Merriman, P. Gordillo, J. Connell, A. Elfaraskoury, B. Echeveste

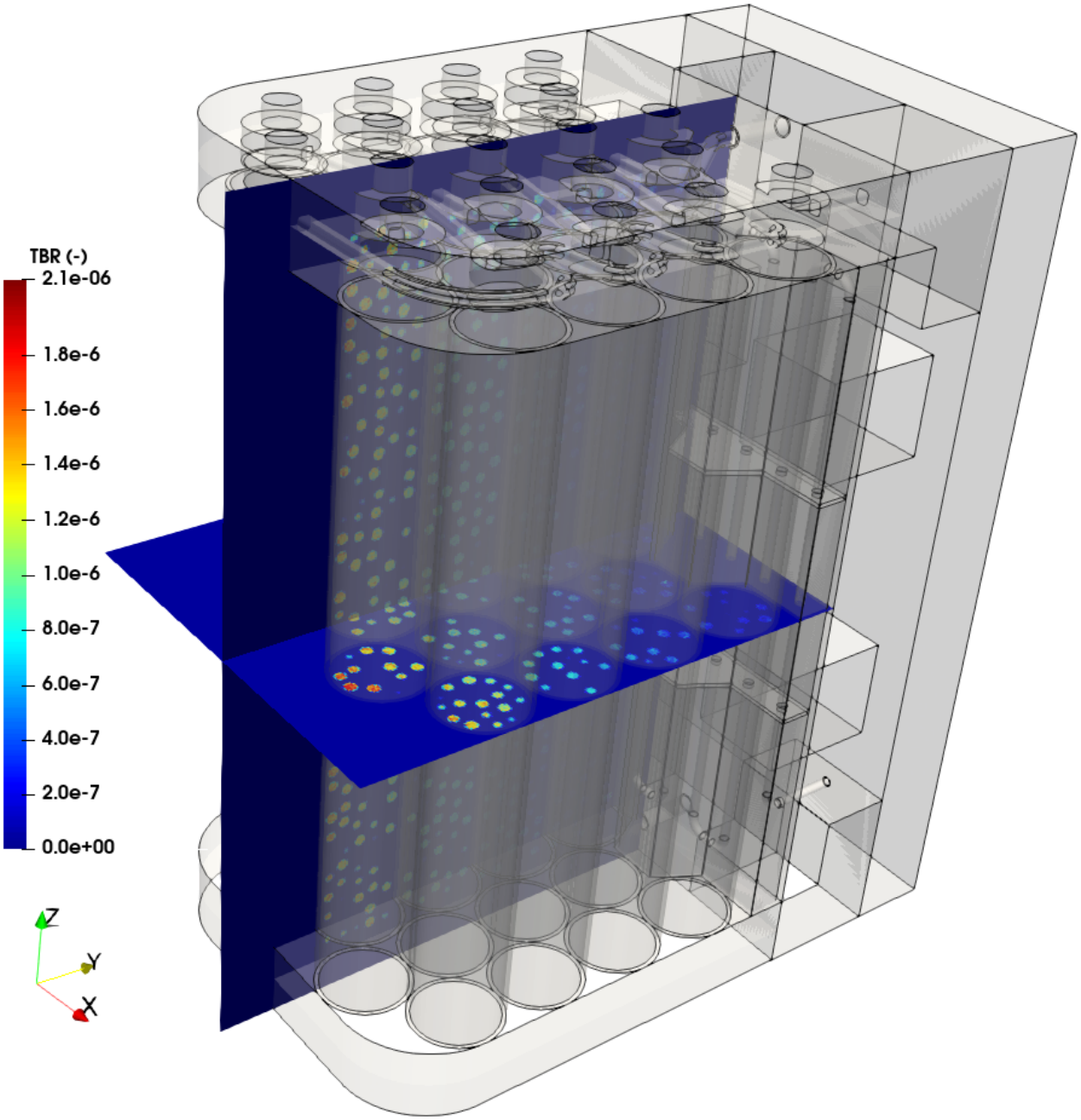

Figure 1: Tritium Breeding Ratio (TBR) distribution in the proposed pebble encapsulated breeder blanket design for the STEP programme. Tritium is generated in inside the encapsulated FLiBe and extracted through the pebble shell to poloidal gas cooled pipes.

Highlights

Encapsulated breeder commercial blanket conceptual design

J. Fradera, S. Sadaba, F. Calvo, S. Ha, S. Merriman, P. Gordillo, J. Connell, A. Elfaraskoury, B. Echeveste

- A breeding blanket option for STEP is presented.
- A breeding blanket design with encapsulated breeder material is exposed.
- The presented study is a first decided step towards a commercial blanket.
- An design methodology is followed to achieve a working conceptual design.
- A neutronic sensitivity to component thickness and materials is shown.
- A thermal hydraulic analysis of a pebble and a packed bed is presented.
- A design with a TBR> 1.1 is achieved.

Encapsulated breeder commercial blanket conceptual design

J. Fradera[a,1,**], S. Sadaba[a,**], F. Calvo[a], S. Ha[b,2], S. Merriman[b], P. Gordillo[c], J. Connell[c], A. Elfaraskoury[a], B. Echeveste[a]

[a] *IDOM, Derbyshire, Cromford Mills, Mill Lane, Matlock, DE4 3RQ, United Kingdom*
[b] *UKAEA, Culham Science Centre, Abingdon, Oxfordshire, OX14 3DB, United Kingdom*
[c] *Nuclear AMRC, University of Sheffield, Advanced Manufacturing Park, Brunel Way, Rotherham, S60 5WG, United Kingdom*

Abstract

As part of the UKAEA Spherical Tokamak for Energy Production (STEP) fusion power station programme, a novel breeding blanket design was assessed. A conceptual design of STEP, which will be an innovative plan for a commercially-viable fusion power station, will be completed by 2024. The final aim of the current assessment is to find a conceptual design that can be manufactured with existing techniques without compromising the fuel self-sufficiency, the heat removal and the shielding functions. The proposed design is based on encapsulating the breeding material into pebbles of a gas cooled packed bed. The generated tritium in the breeding material, as well as Helium, will be extracted from the pebbles and directly removed from the blanket by the cooling gas. A frontal multiplier as well as a back reflector have also been studied to maximize the tritium generation. This paper, which is a decided first step towards a possible commercial breeding blanket for STEP, covers the material design properties and their compatibility, the design configuration, the neutronics analysis, the thermal-hydraulics analysis, a preliminary structural analysis, safety aspects and waste segregation and disposal.

Keywords: Fusion, STEP, breeding blanket, encapsulated fuel, tritium, self-sufficiency, thermal-hydraulics, mechanical, neutronics, FLiBe

Glossary

Abbreviations

NAMRC	Nuclear Advanced Manufacturing Research Centre
BB	Breeding Blanket
BC	Boundary Condition
CFD	Computational Fluid Dynamics
DCLL	Dual Coolant Lithium Lead
EBW	Electron Beam Welding
FW	First Wall
HCLL	Helium Cooled Lithium Lead
HCPB	Helium Cooled Packed Bed
HT	High temperature (above 450 C for Eurofer 97)
HTC	Heat transfer coefficient
IPFL	Immediate Plastic Flow Localization
LT	Low temperature (below 450 C for Eurofer 97)
MCNP	Monte Carlo N-Particle
MHD	Magneto Hydro Dynamics
NHD	Nuclear Heat Deposition
STEP	Spherical Tokamak for Energy Production
TBR	Tritium Breeding Ratio
UKAEA	United Kingdom Atomic Energy Agency
VOF	Volume of Fluid
V	Fatigue usage fraction

Greek characters

ϵ	void fraction
ϕ	Neutron flux

Latin characters

e	FLiBe fraction
H	nuclear heat deposition
Q	tritium or other hydrogen isotopes
T	temperature

Subscripts

x, y, z	coordinates

1. Introduction

The UKAEA Spherical Tokamak for Energy Production (STEP) is an innovative plan for a commercially-viable fusion power station. A conceptual design of the reactor is foreseen to be completed by 2024. Within this programme, one of the key components to be developed is the breeding blanket, which provides shielding from the fast neutrons (~14MeV) generated in the plasma, extracts heat for power generation and breeds tritium (Q) to achieve the self-sufficiency principle. This work presents a conceptual design of a possible breeding blanket for STEP focusing on the mentioned blanket functions and especially on the manufacturability with available techniques.

It must be noted that the assessment has focused on a commercial breeding blanket concept, so a balance between high

*corresponding author
**both authors have contributed equally to this work
[1] contact: jorge.fradera@idom.com
[2] contact: samuel.ha@ukaea.uk
[3] contact: pablo.gordillo@namrc.co.uk

performance materials, commercially available and reduced cost materials has been sought. Despite of the mentioned compromise to focus on a commercial breeding blanket, the presented concept allows different breeding materials, even exotic ones, to be used and ensures self-sufficiency, safety and a high thermal efficiency for a high volumetric power density.

A series of sensitivity analyses (see Sec. 4) have been carried out to both assess the feasibility and the performance of the proposed concept and to improve the layout. This paper exposes the conceptual design excluding any optimization of the blanket dimensions and aims to be a first decided step towards a commercial breeding blanket for the future STEP power station.

2. Methodology

The applied methodology for the design of the encapsulated breeding blanket concept is based on a thorough analysis of previous blanket concepts, a series of constraints intrinsic to the blanket functions and on splitting the functions of the blanket. In addition, lessons learned from other blanket projects have been implemented.

Previous blanket concepts can be divided into two main categories: liquid, e.g. HCLL [1] and DCLL [2], and solid blankets , e.g. HCPB [3] among many others. Liquid blankets have thermal-hydraulic and material compatibility problems, e.g. MHD and corrosion among others, as the coolant is usually the breeder. Solid concepts have Q extraction and structural problems, e.g. high Q inventories and swelling among others. These concepts have extensively been studied and optimized resulting in complex, complicated, difficult to manufacture, expensive and difficult to inspect components.

The present design can be understood as a hybrid between both categories where the best of each technology has been implemented.

The main blanket functions are the following:

- Shielding from fast neutrons (~14MeV) generated in the plasma.
- Heat extraction for power generation.
- Tritium production to achieve the self-sufficiency principle.

The blanket uses the multiplier, the structural material, the breeder material and the reflector to provide shielding. In addition, a high Tritium Breeding Ratio (TBR) also ensures that most of the neutrons that get to the blanket are absorbed. This function is therefore distributed among the blanket components.

The heat extraction has to be carried out by a working fluid. The selected fluid is a gas like in the HCPB concept. Pumping requirements and heat transfer capabilities involve pressurized gas coolants. Therefore, the blanket shall include pressure components that can be easily manufactured, installed, welded and inspected. One of the most common and appropriate geometries that can withstand the working pressure of the coolant, which is >1MPa is a cylindrical pipe.

Tritium production in fusion reactors is achieved by means of the $Li^6(n,\alpha)H^3$ and $Li^7(n,n'\alpha)H^3$ reactions. As far as the authors know, in all blanket concepts the generated Q diffuses through the breeder material and eventually degasses as Q_2. Note that some blanket designs use water, so the desorbed species would be then Q_2O. Note also that the desorbed species can be a combination of hydrogen isotopes if isotopic exchange is used to enhance de estraction. This complex phenomenon has a huge impact on the Q cycle of the reactor because Q shall be recirculated to become the plasma fuel again.

Solid breeder blanket concepts usually accumulate Q in the breeding material which becomes an issue from the safety point of view. Furthermore, He is generated at a similar rate as Q, so nucleation is expected resulting in material swelling. This phenomena makes the Q extraction and recirculation a challenging issue. Blanket concepts like the HCPB need heating cycles above the operating temperature to extract the Q from the breeder.

Liquid breeder blanket concepts usually have low Q solubilities [4], so extracting Q is more efficient and no swelling is expected in the breeder material. However, He do also nucleate and accumulate in the cooling system (see, e.g., [5, 6, 7]). As a result, Q can be trapped in the He gas pockets. In addition, the He pockets reduce the heat transfer significantly, which mey pose a problem from the structural point of view.

The proposed blanket decouples the cooling function from the breeding one by allowing gases to flow through as the breeder is encapsulated in a pebble. The breeder material is then chosen to be liquid in order to extract the Q more efficiently. The He issue is then coupled to the Q extraction by allowing gasses flow through the pebble shell while the breeder is kept inside.

Multipliers are needed to achieve high TBRs. This function has also been partially or totally decoupled from the breeding and cooling functions by placing the multiplier material outside the pipes that hold the pebbles packed bed and allow the coolant flow. It must be noted that this decoupling implies the use of materials that are vacuum compatible and that degasses neither Q, nor He. Note also that if FLiBe is selected as the breeder, the multiplication effect is embedded into the breeding function. Then, in this case, the Q generation through the $Be^9(n,2n)Li^7$ nuclear reaction follows the same extraction process as that for Li.

Once the functions were decoupled as much as possible, a series of sensitivity analyses were performed to asses each function separately.

3. Configuration

A selection of materials is briefly exposed in the present section as a result of a more extensive analyses carried out within the UKAEA breeding blanket design project. Note that safety issues regarding the material selection are presented in Sec. 4.5.

The proposed blanket is based on encapsulating the breeder into pebbles of a gas cooled packed bed. A top and bottom manifolds connected by vertical pipes allow the packed bed cooling by means of a gas. A frontal multiplier together with a multiplier pebble bed among the pipes and a back reflector are implemented to improve the neutron economy and allow TBRs>1.

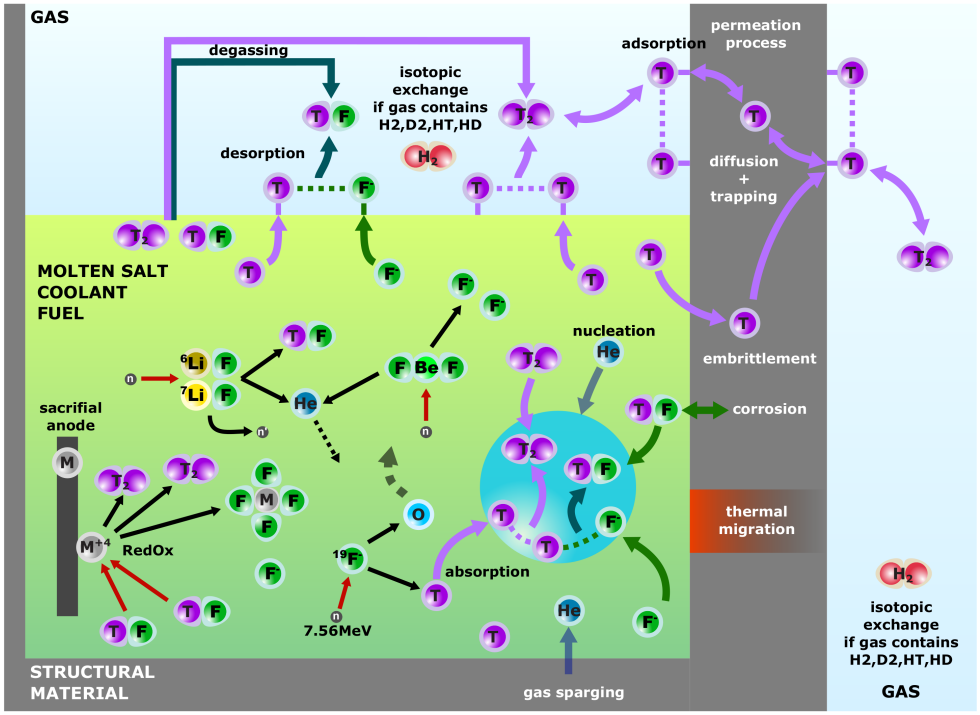

Figure 2: Summary of Q transport in FLiBe.

The concept is "dual coolant": the carrier gas (to transport Q) and the coolant gas (to cool down the structures) are the same gas circuit.

3.1. Encapsulated breeder

As has already been mentioned, several breeders can be used (see e.g. [8]) with the proposed design with very little modifications as the material is encapsulated inside a pebble. For the present work FLiBe (Li_2·BeF_4) [9] has been selected as the breeder material. Note that other blanket concepts that use this molten salt exist, e.g., the ARC reactor [10] or the US APEX programme [11]. FLiBe has a high TBR and neutron multiplication capability close to liquid breeders like $Pb_{17}Li_{83}$ as exposed in [12] and references therein. FLiBe has a X-eutectic, with 0.328% Be and a melting temperature of 458.9ºC, and an eutectic, with 0.531% Be and a melting temperature of 363.5ºC. The highest the Be concentration the lowest the viscosity, which is a critical parameter regarding the thermal-hydraulics of a liquid breeder blanket. For the presented concept, as the FLiBe will be encapsulated, the viscosity may only affect the He nucleation onset with very little impact on the behaviour of the Q extraction. Note that Q transport in FLiBe systems is rather complex as shown in Fig. 2. However, a low melting temperature is preferred to work in the temperature window of the structural materials. Therefore, if a high Li content is used, the pebbles will have to be thermally isolated and withstand temperatures above the structural material limit. Alternative breeders in [13] include LiF-LiI-LiCl molten salts, with triple eutectic points down to 340ºC.

The generated Q and He in the FLiBe will eventually nucleate generating a gas pocket. To enhance this process the pebbles are designed so a coolant gas pocket is included in the pebble. Therefore, both Q and He will degas to the pocket after diffusion or nucleation.

The decoupling of the cooling from the breeding function and the adoption of a pebble rises the following issues:

- Q and He extraction from the pebble.
- FLiBe operating temperature window.
- FLiBe material compatibility.
- Pebble shell operating temperature window.
- Pebble heat removal.

The Q extraction can be achieved either by diffusion through a metallic shell or by porous diffusion through, e.g., a ceramic one. The former is a slow process that can be limited by surface phenomena and the latter involves a pore size small enough to prevent FLiBe leakage. When He generation is accounted for, the porous shell solution becomes the only viable option. Otherwise He will accumulate and pressure build-up will eventually lead to an structural integrity problem or it will force the blanket to be removed from the reactor.

Regarding the FLiBe operating temperature, the porous shell, made, e.g., of a ceramic material like Silica, porous graphite or SiC, will have a lower conductivity than that of a metallic shell,

so it can be used to increase the operating temperature window of the FLiBe.

FLiBe is know to corrode structural materials, especially if Q is generated. Dissolved hydrogen, or any of its isotopes, in FLiBe exists in atomic form. A RedOx reaction between Q and F determines the existence of QF, which is very corrosive. If QF exists in the FLiBe it can corrode a metallic shell or it can be extracted along with Q and He to the coolant stream posing a major problem to the primary coolant circuit. In both cases the generation of QF must be prevented. A small amount of metallic Be can shift the RedOx reaction so Q is desorbed in its molecular form Q_2. Other metals like Zr could be used as RedOx controllers, but then activation might become a problem.

The use of a porous shell comes not only with a structural problem, but also with a dust generation issue. The present concept uses a metallic jail made of structural material around the porous shell to prevent the contact among pebbles, withstand the weight of the packed bed and allow deformations due to mechanical loads. This jail poses no significant impact on the extraction or cooling of the pebbles.

The pebble design is as follows:

- Molten FLiBe as breeding material.
- Metallic Be as RedOx controller to prevent the generation of QF.
- A coolant gas pocket to allow pressure changes and, Q and He degassing.
- A ceramic porous shell that allows Q and He extraction, prevents FLiBe leakage and allows the FLiBe operating temperature window.
- A metallic jail that prevents contact among pebbles and ensure the structural integrity of the packed bed.

Another key aspect of breeders is the MHD and magnetic loading on metallic structures, which may causes high pressure drops, low heat transfer coefficients in liquid blankets and structural integrity issues. In the present design MHD load are restricted to the encapsulated FliBe, where MHD effects are low (see e.g. [10]) and where the metallic shell and pipe layout can be designed to minimize any effect. Note that if a ceramic non-conducting material is used, the MHD are dramatically minimized.

3.2. Cooling system

Many coolant options exist for breeding blankets. Either the breeder material is the coolant (dual concept) or a liquid (e.g. water) or a gas (e.g. He) is used. The use of a liquid coolant was discarded to prevent in-box LOCA events as well as due to chemical compatibility and Q extraction. Among the cooling gasses, He is the best one as is transparent to radiation and has very good heat transfer capabilities. However, as the study focuses on a commercially viable solution, He is not the preferred options as it is a very scarce gas with a high market price. In addition, He requires a large pumping power and operating pressures above 7MPa. Therefore, a compromise between activation and heat transfer capabilities was sought.

Nitrogen (N^{16}) is known to have a significant interaction with thermal neutrons (see [14]) and is even used as a shut-down gas for gas cooled reactors. However, it is a very cheap gas that requires lower pumping requirements than He and works with conventional power generation technologies. Some reactor concepts using N_2 or even air as coolant in a direct power generation cycle exist (see [15] among others).

3.3. Multiplier

On one hand, there exist many concepts where either Be or a Be compound is used. Be has a high multiplication factor, but it generates Q through the generated Li by the $Be^9(n,2n)Li^7+H^3$ nuclear reaction for >10.5MeV. Pure metallic Be and Be compounds like Be_{12}Tihave the same issues as the breeding ones as a sweep gas is needed to remove Q, the accumulated Q inventory reduced the operating time of the blanket and swelling is also expected to be a major issue [16].

On the other hand, Pb is also used as a multiplier as $Pb^{208}(n,2n)Pb^{207m}$ for >7.4MeV. One advantage of using Pb is that no carrier gas is needed as no Q is generated. However, more multiplier is needed to achieve the same multiplication factor as that of Be and the low melting temperature of pure Pb (327.5ºC) may be a problem. Several lead compounds, e.g. the inter-metallic Zr_5Pb_4have been proposed, but they are scarce or difficult to synthesize with the available technology as far as the authors know..

The present design proposes the use of a Pb compound to prevent the use of Be, which is scarce, toxic and generates Q. A good candidate would be Zr_5Pb_4, but a compound with a lower content of lead like PbS may be a better option as it is abundant and has a low price when compared to all the aforementioned multipliers. PbS has a high melting point so it can be placed between the coolant pipes as a pebble bed.

3.4. Reflector and shielding

The use of a reflector to improve the neutron economy of the blanket and generate more Q is also a good option to reduce the total thickness of the blanket. Low Z reflectors like boron or graphite are know to be efficient reflectors for thermal reactors. However, the neutron energies of a fusion reactor are too high for this reflectors to work properly. High Z reflectors work better for fast neutrons, but they might not be efficient for scattered neutrons generated by the multiplier and the breeder. As a result, compound like tungsten carbide (WC) or tungsten boride (WB), which have good mechanical properties and vacuum compatibility, can be used to cover the range of neutron energies for both shield the back of the blanket and increase the TBR. Note also that these materials have good thermo-mechanical properties [17] and are very common for tooling, so their availability and cost is not an issue.

3.5. Layout

The layout of this blanket concept is mainly driven by the aforementioned decoupling of functions, which led to the pebble design to be the key component. The blanket design can be summarized as shown in Table. 1. A pebble design example is

Function	Material	Configuration
Structure	Eurofer 97	Electron Beam Welding (EBW)/ milling
Cooling	N_2	Top and bottom manifold with vertical pipes in between
Breeder	FLiBe	Encapsulated in a porous ceramic shell protected by a metallic jail
Multiplier	PbS	Packed bed among pipes

Table 1: Materials and configuration of the encapsulated breeder blanket.

shown in Fig. 3. Further optimization of the design will lead to optimum thickness for the pebble to degas Q and He as well as to operate in the desired temperature window without leaking FLiBe. The pebbles are slightly loose packed (ϵ=0.45) into

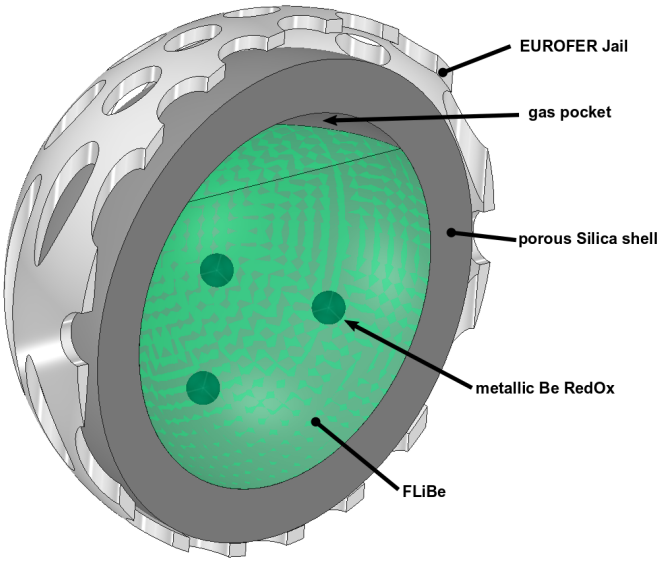

Figure 3: Example of a pebble design for the encapsulated breeder concept.Sizes are not to scale to show the different components.

the pipes to allow expansion as shown in Fig. 4. Note that the jail, together with the loose packing will allow a better cooling of the system. Contrary to some well-known designs (WCLL, HCPB), the FW structure is detached from the BB. Top and bottom manifolds (see Fig. 5) distribute the flow. The distribution pattern can be optimized to enhance heat transfer, keep the blanket within the working temperatures and for the baking process before operation.

3.6. Structure

3.6.1. Structural material

The maximum thermal efficiency of the blanket is determined by the maximum operational temperature of the structural materials. The selection of the structural material for pipes, manifolds and supports is mainly driven by its activation and its performance at high temperature.

For the materials of interest, most benefit is obtained if we work in the creep regime, avoiding cyclic thermal stress. Indeed, undesirable cyclic loads are penalising the creep regime through the well-known creep-fatigue interaction and progressive deformation.

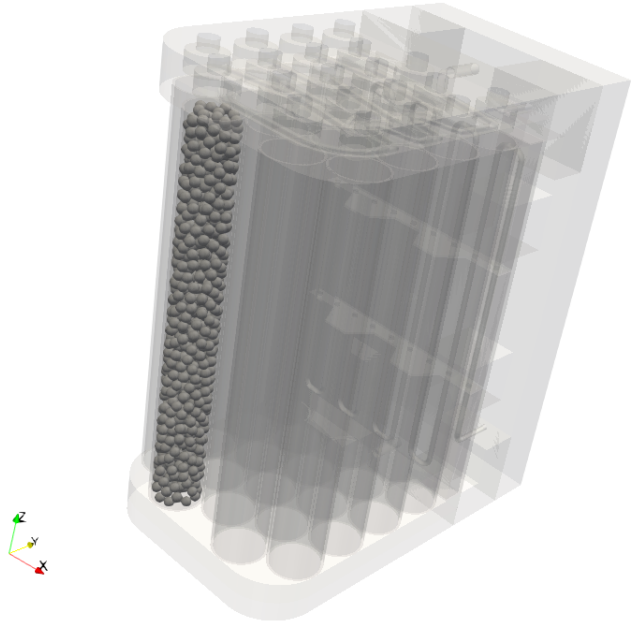

Figure 4: Packedbed inside one of the cooling pipes.

If the material temperature is reduced (i.e. cold supports, reduced thermal performance), then embrittlement irradiation effects under instantaneous loads (IPFL failure) becomes dominant.

Several materials RAFMs (Reduced Activation Ferritic Martensitic steels) were considered: Eurofer 97, MHT-9, ODS, F82H and ORNL 9Cr-2WVTa. Regarding activation, the lower the Mo, Nb, Ni and Cu content the better. It can be concluded, then, that Eurofer 97, F82H and ORNL 9Cr-2WVTa are the best candidates. When cost and availability for STEP are accounted for, Eurofer 97 seems to be the best option as its mechanical properties allow a temperature window from 300ºC to 550ºC; for the present work Eurofer 97 was selected.

The material allowables for Eurofer 97 are compiled in Tab. 2. Note that the critical properties here are based on [18], although HT rules (creep) and LT rules under irradiation (IPFL) are still under discussion [19] [20] [21].

3.6.2. BB structural concept

The pebbles are designed to leak gases generated inside, while retaining the fluid. As a result, no significant internal pressure is built. Additionally, the jail supports the self-weight and inertial loads of the system, leaving very low structural requirements for the pebble shells.

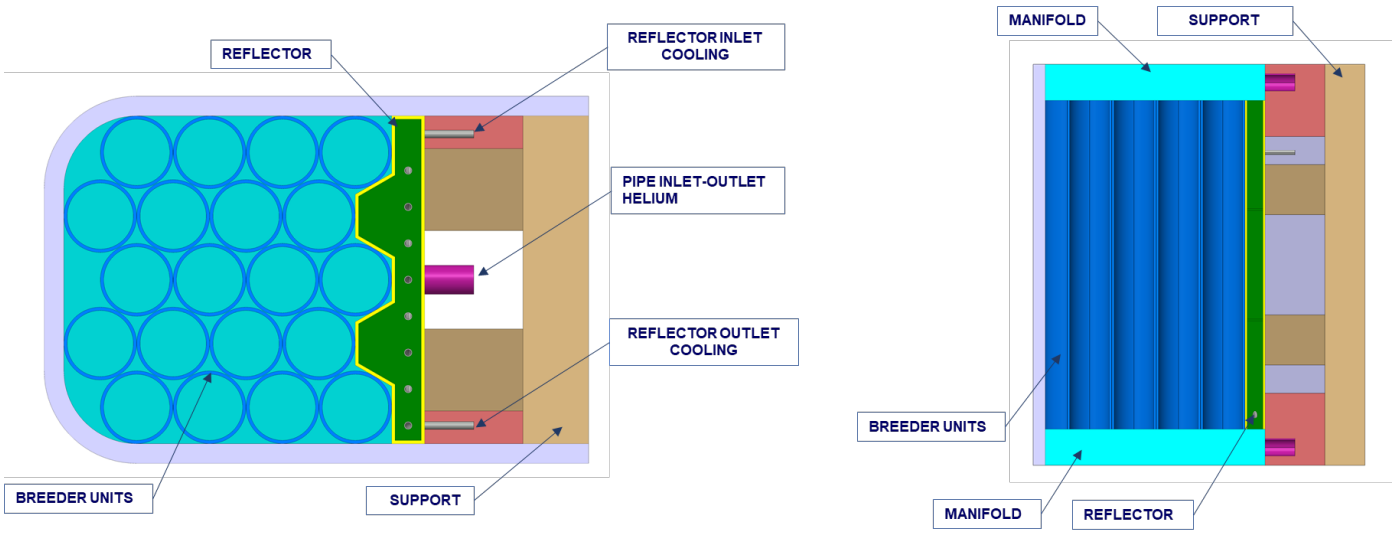

Figure 5: Preliminary blanket design with the vertical pipes in-between manifolds.

Temperature	**Creep@3 years**		**Immediate Plastic Collapse**		**Immediate Plastic Flow Localization**	
	$V = 0$	$V = 0.2$	Level A	Level C	Level A	Level C
(ºC)	$S_t \cdot W(S_t, 0)$	$S_t \cdot W(S_t, 0.2)$	S_m	S_m^C	S_e	S_e^C
350	∞	∞	165	223	260	324
450	159	31	145	196	526	656
500	115	23	131	177	659	824
550	74	14.8	113	170	659	824

Table 2: Some relevant allowables [MPa] for Eurofer 97 following [18]. Fatigue usage fraction V is postulated as V=0 (unfatigued) or V=0.2 (20% fatigue)

The jails shall withstand a high temperature with possible thermal cycles in the pebble bed causing progressive deformation and fatigue, being the main concern the effect of fatigue cycles in the creep resistance. Note that the creep-fatigue interaction lowers significantly the allowable membrane stress under constant loads (gravity). Therefore, the pebble bed shall be loose enough to accommodate changes in pebble geometry (no "local" thermal overconstraint) the following provisions shall be ensured:

- Provision to nominal dimensions and tolerances: the pebble bed diameter tolerances and the pipe inner diameter cannot be packed in a horizonal plane, avoiding 2D-like locking in the pipe section.
- Provision to volumetric expansion: the pebble bed expands in the axial direction of the pipe. Then, the distance to the pipe end shall be sufficient to accommodate a pessimistic expansion case, at least in most of the working cycles producing fatigue

Note that EM loads and thermal loads are opposite design drivers: EM loads require stiff structures, while thermal loads work better with unconstrained structures. The pipe-manifold structural topology releases some structural constraints to enhance thermal behaviour, but EM behaviour can be compromised. To this aim, the structural topologies in Tab. 3 were assessed. Note that free supports do not exist in practice, since they are not able to withstand any EM load. However, the concept is very useful for the thermal design: they constitute the best possible scenario for the thermal stress, and help estimating the engineering effort for the design of the supports.

Config.	**Blanket**	**Supports**
PU	Pipes with manifolds	Free
PC	Pipes with manifolds	Fixed
HU	Honeycomb	Free
HC	Honeycomb	Fixed

Table 3: Structural topologies for analysis.

Recall that some concepts (WCLL, HCPB) use a box structure, which is very stiff, while the pipe-manifold is more compliant. An intermediate solution is a honeycomb structural concept. Also, hybrid structures between mixing pipe-manifold and honeycomb-like may arise in further optimization exercises.

An important aspect of the presented design is the low mass of structural material when compared to other existing blankets, since more efficient structures (pipes vs plates) have been used. This has a significant impact on the amount of activated material as well.

4. Analyses

A series of analyses have been carried out to assess the feasibility of the design and improve the conceptual design. In addition, especial care has been taken to decouple as much as possible the analyses. The applied methodology consists of the neutronic calculations as the first step so as to understand the impact of the geometry and the materials on the performance of the blanket. Once a baseline case was chosen, a single pebble thermal-hydraulic and Q transport analysis is carried out. As the final stage, the packed bed was modelled. The mechanical loads on the baseline case (with a range of thermal assumptions) were then assessed for the pebble and the main structural components. Note that further analyses, which are out of the scope of the present study, are needed to achieve a more detailed and optimized design.

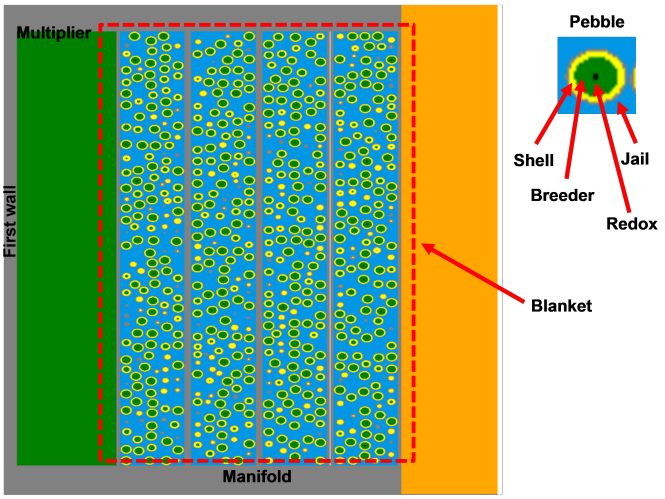

Figure 6: OpenMC simplified 3D geometry slice for the blanket analysis showing the pebbles in each pipe.

4.1. Neutronics

The neutronic analyses were performed for >120 cases and error below 5%. The CAD geometry was translated into an OpenMC© parametric geometrical model as shown in Fig. 6 where components thickness and material distributions could be changed. The pebble packed bed was generated with the OpenMC© packing generator and the TRISO model. The TBR of a blanket depends on the geometrical parameters of components of the blanket as well as on the materials of these components. Therefore, a multi-parameter optimization problem must be solved for a TBR>1. In order to reduce the amount of analyses, the problem has been split in two: the geometrical optimization and the material optimization. This methodology assumes that the effect of the materials on the sensitivity analysis of a given geometrical parameter does not change from the tendency standpoint. This fact is also checked during the analysis of the sensitivity to the materials results.

4.1.1. TBR sensitivity to components thickness

A sensitivity analysis to the parameters shown in Table. 4 was performed assuming $Be_{12}Ti$ as multiplier, WC as reflector, Eurofer 97 as structural and jail material, Silica for pebble shell and metallic Be as the redox controller of the breeder material, which is FLiBe (enriched to 95% Li^6). The coolant was selected to be N_2 and the blanket space among pipes was left to be vacuum. The packing void fraction of the pebbles was kept low at 0.45 to save computational time. As a result, low TBR were expected, but the difference between the use of geometrical parameters was significantly be augmented.

First Wall(cm)	2	4	6
Frontal multiplier(cm)	3	6	9
Manifold(cm)	1	5	10
Reflector(cm)	5	15	20

Table 4: Thickness of components matrix for the sensitivity analysis.

The effect of changing the FW thickness is straight forward; the thicker it is the lower the TBR is achieved as there is more shielding (see Fig. 7). The effect of changing the frontal multiplier follows the same tendency as the First Wall (FW), having very little impact on the TBR. Therefore, this result suggests that the multiplier distribution can be optimized leading to an increase in the TBR and possibly a blanket thickness reduction.

The effect of changing the manifolds is interesting as it follows a different tendency than the FW. The thicker the manifold the higher the TBR. It could be though that the manifolds will shield the breeding zone and prevent the addition of more breeding material. However, a multiplication effect can be observed. Obviously, there is a limit thickness where the reduction of the breeding material is not compensated by the multiplication effect of the structural material of the manifolds. This effect allows a thicker and simpler to manufacture manifold as well as more room for optimization.

The impact of the reflector on the TBM is almost negligible as it works as a shielding rather than as a reflector. The same TBR is achieved for different reflectors thickness. This result suggests that the reflector should be included elsewhere if the neutron economy is to be improved.

4.1.2. TBR sensitivity to component materials

A TBR and a Helium Breeding Ratio (HeBR) sensitivity to different materials was performed assuming a 2cm First Wall, 6cm for the manifolds, 10cm for the reflector and a variable multiplier thickness to check the material independence with respect the previous sensitivity analysis. Note that these thickness were selected to freeze the some parameters and see only the effect of the materials. Note that in this analysis the space among pipes was filled with the multiplier.

The highest TBR cases were selected (see Fig. 8) as potential cases for optimization. Both Be and Pb based multipliers achieve TBR>1, but, only Pb based multipliers at the front improved the TBR. Beryllium is a scarce material that has been the object of several studies to reduce its content in blanket designs(see, e.g., [22]). In addition, its handling is very danger-

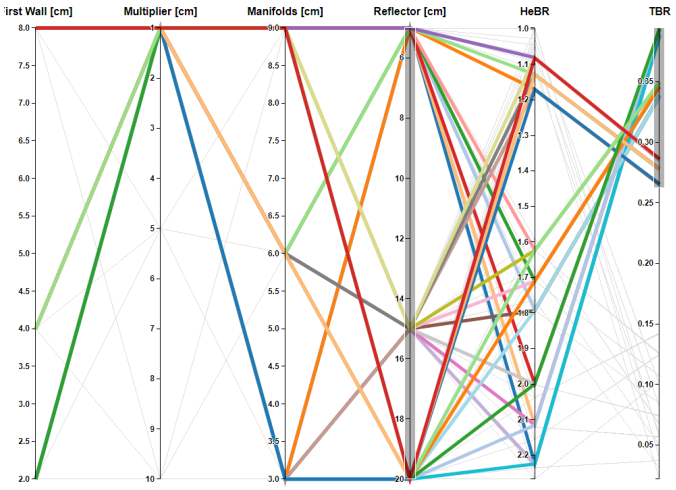

Figure 7: Analysis of the TBR sensitivity to different component thicknesses.

Frontal multiplier material	$Be_{12}Ti$	Lead	Zr_5Pb_4
Multiplier(cm)	1	5	10
Blanket multiplier material	$Be_{12}Ti$		Zr_5Pb_4
Reflector material	SiC		WC

Table 5: Materials of components matrix for the sensitivity analysis.

ous, so a "Be-free" blanket seems a better option than a Be one. Regarding the reflector, it looks like both WC and SiC have similar TBRs, but HeBR is lower for SiC

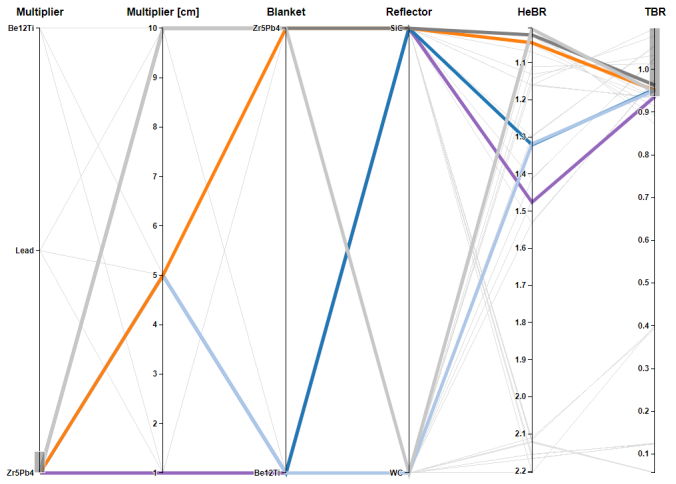

Figure 8: Analysis of the TBR sensitivity to different materials.

4.1.3. Detailed analysis of the base line case

Following to the exposed neutronic analysis, a detailed analysis of the Zr_5Pb_4based model with SiC as reflector was selected as a base line case in order to detect optimization features. The selected size of the components was changed until a TBR~1.1 was achieved.

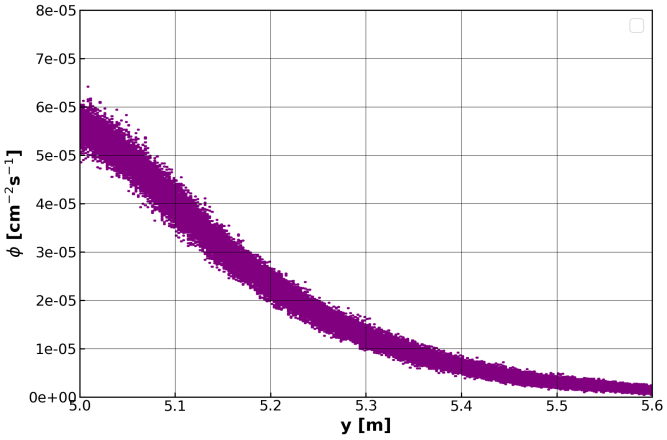

Figure 9: Neutron flux profile for an equatorial slice.

The neutron flux is shown in Fig. 9. The expected exponential decay is observed across the blanket, dropping two orders of magnitude at the back of the reflector region. It must be noted that most of the flux is located between the FW and the second row of pipes. This suggests that the blanket can be optimized by allowing more multiplier among the pipes and less thickness at the front region.

The resulting nuclear heat deposition is shown in Fig. 10 for a first wall neutron flux of $2{\cdot}10^{14}$ n·cm^{-2}·s^{-1}, Note that neutron rates in a compact spherical tokamak can reach up to $1{\cdot}10^{19}$ n·s^{-1} (see [23] among others). The peak $\boldsymbol{H}$ reaches a value of 14.8MW/cm^3 at the breeder material. The structural material at the front of the blanket reaches power depositions arround 1MW/cm^3 falling to 0.001MW/cm^3 at the back of the blanket. As a result, it can be concluded that the back reflector in the present configuration may not need active cooling. Furthermore, the nuclear heating in the pebbles can be easily optimized for the working temperature of the FLiBe.

The Q generation only occur inside the pebbles (see Fig. 12) as no Be based multiplier was used. The cooling pipes should extract all the Q, so no carrier would be needed elsewhere. The TBR follows the neutron flux tendency as expected and shown in Fig. 11. The cooling pipes at the back of the blanket have a very small TBR, but still significant. Note that most of the neutrons are shielded by the FLiBe in the pebbles.

Both the TBR and the HeBR follow an exponential decay. The discrete locations of the breeder generate a wide dispersion of the results. The HeBR is slightly higher than the TBR as helium is also generated in the structural material and the multiplier. However, the difference is very small. It can be observed as well that the HeBR is slightly higher in the first wall than in the multiplier. The helium generation poses a problem if it is generated inside the multiplier as swelling might damage the blanket. In this case, the generated He is low enough so no significant swelling is expected.

It can be concluded that the current design allows further improvement to achieve higher TBR as well as to minimize neutron leakage. Therefore, the design seems feasible from the

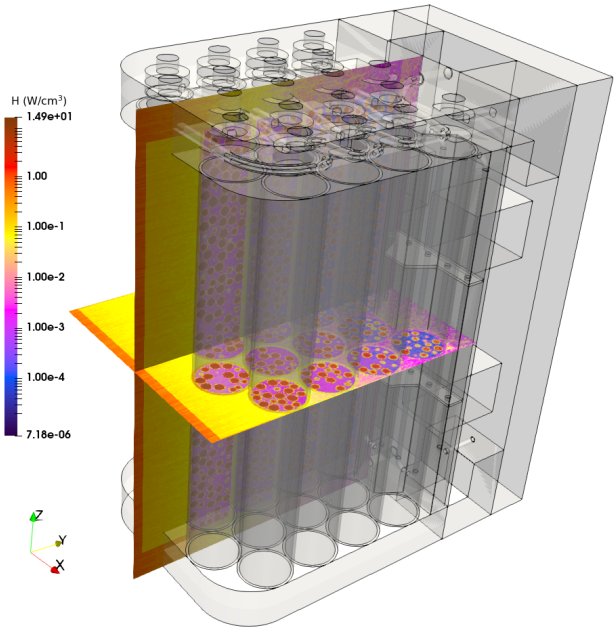

Figure 10: Nuclear heat deposition distribution.

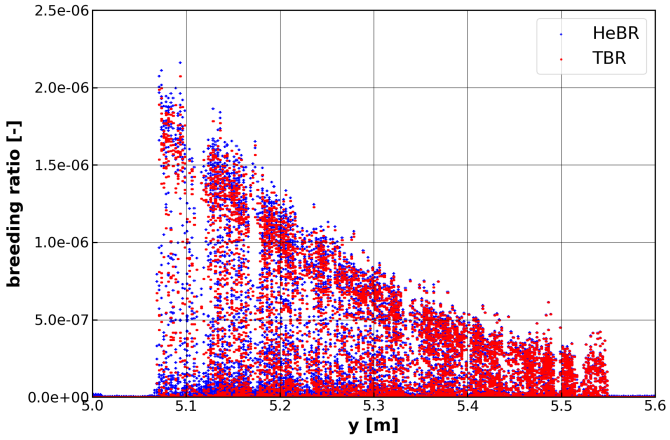

Figure 11: TBR and HeBr profile for an equatorial slice.

neutronics point of view.

4.2. *Thermal-hydraulics and Q transport*

For a preliminary thermal-hydraulic analysis, two models were generated, a single pebble that included the shell, the breeder and gas pocket, and a full pipe model including the packed bed with the exact pebble distribution as that in the neutronic calculations.

4.2.1. *Pebble model*

A single pebble multiphase model was generated to assess the internal thermal hydraulics and Q transport in the FLiBe and the gas pocket. The model was run as a unsteady case with the Volume of Fluid (VOF) method using the CFD software STARCCM+®until a steady state was reached. The heat source and Q generation terms were extracted from the neutronic baseline case results corresponding to a pebble in a front pipe. The FLiBe properties were chosen to be temperature dependent from [24] and the gas in the pocket was modelled as an ideal gas. The external surface of the shell was set to a constant temperature corresponding to the average temperature window.

The steady state solution shows that the internal relative pressure slightly changes due to the movement of the FLiBe-Shell interface. The interface stays stable with very little change over time due to the formation of a toroidal vortical structure around the FLiBe region as shown in Fig. 13. These vortical structure pushes the FLiBe up from the center of the sphere towards the gas pocket. The FLiBe sweeps the interface and goes downwards by the pebble internal walls as the salt is cooled down. Therefore, a convective cell is formed inside the pebble enhancing heat and mass transport through the shell.

The temperature distribution in the FLiBe (see Fig. 14) shows how the gas pocket has a significant gradient as well as the highest temperature. The shell stays almost at the coolant temperature.

The Q concentration in FLiBe can be assumed to be constant, as very little differences is noticed (see Fig. 15). Most of the Q is trasnported to the gas pocket and accumulates at the top of the pebble. The toroidal convective cell removes the Q from the bottom of the pebble and pushes it to the gas pocket.

4.2.2. *Packed bed model*

Once the pebble analysis was completed, the packed bed was studied. The pebble packed bed can be generated with three methods. The first method consists of running a soft body simulation with STARCCM+®. The resulting packed bed is very realistic, but lacks the conformality with respect the neutronic simulations and is computationally intensive. The second method involves a rigid body simulation (see Fig. 16), which is computationally less demanding (see [25] and references therein), but has the same conformality problem as the spheres will not match the location of the neutronic simulation pebbles. The third method is to use the coordinates of the center of the pebbles in the neutronic simulation and translate the geometry with a custom script into STARCCM+®. Note that the previous methods can be used in advance of the neutronic analysis and the geometry be translated to OpenMC© .

A simple thermal hydraulic case with an imposed heat flux at the pipe walls and pebbles, corresponding to that of a front pipe,was setup to assess its thermal-hydraulic behaviour. The coolant was modelled as an ideal gas at an operating pressure of 1 MPa. A constant inlet velocity of U_z = -10 m/s ($\backsimeq$8kg/s) at 573.15 K has been set as boundary conditions.

The heat flux has been extracted as an average value from the neutronic calculations for simplicity . In addition, The inlet and outlet boundary conditions have been extruded to prevent any boundary related numerical instability. Turbulence has been accounted for with the k-ϵ model with corrections for the curvature of the existing surfaces. The generated polyhedral mesh (see Fig. 17) has >100 million cells and a y+$\sim$1 to ensure a

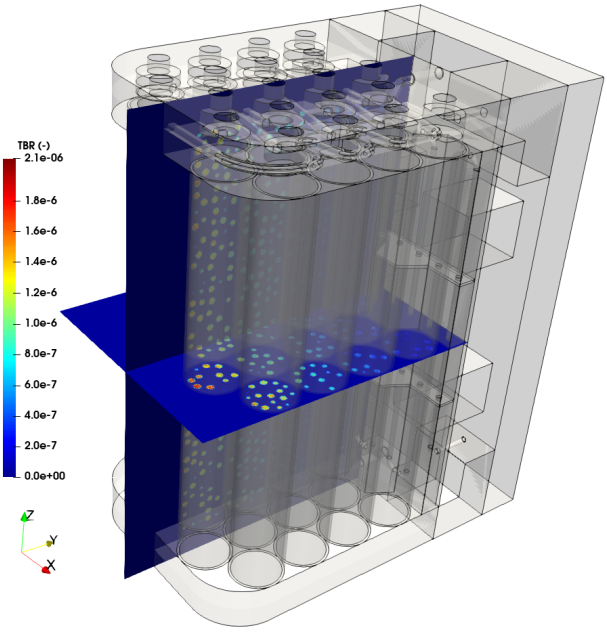

Figure 12: TBR distribution.

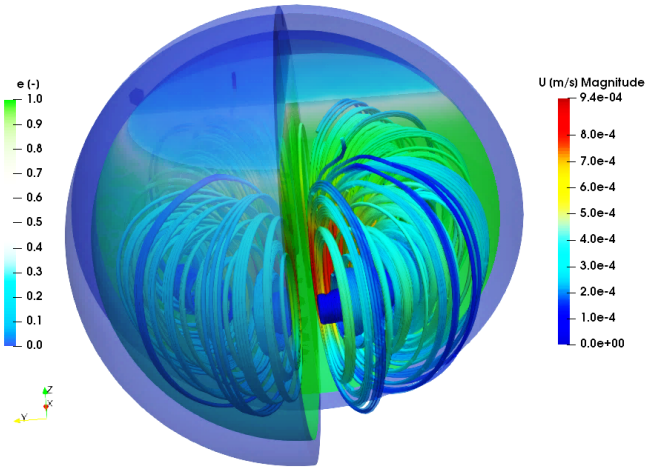

Figure 13: Velocity streamlines (right) in the FLiBe showing the internal convection cell and the FLiBe fraction (left).

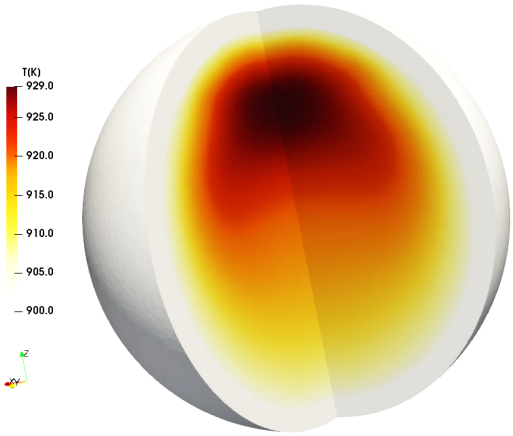

Figure 14: Temperature distribution in the FLiBe showing peak temperatures in the gas pocket.

reliable heat transfer. In addition, a prismatic layer has been included to prevent numerical errors and properly resolve the boundary layer.

The coolant gas, N_2, flows through the core of the packed bed at a lower velocity than that of the region between the pebbles and the pipe walls as shown in Fig. 18. This effect was expected as preferential channels do exist in this kind of packed beds, especially close to the walls. The packing fraction used in this simulation can be improved and the preferential channels reduced by changing the size of the pebbles. This loose packing also accounts for the jail of the pebbles. It must be noted that this phenomenon can be used to cool down the pipes structural material and even the multiplier among the pipes. A closer look at the flow in the packed bed shows a complex flow pattern at the center of the bed. However, the flow distribution is very homogeneous. The two expected stagnation points at the flow impingement and at the other side of the pebbles can be observed in Fig. 19.

Regarding heat transfer, the pipe temperature distribution is shown in Fig. 20. The temperature rises towards the outlet leaving some preferential channels along the pipe with a lower temperature. Note that Nusselt dimensionless number is almost constant due to the high speed of the coolant and the mixing induced by the packed bed. It can be observed that where the pebbles contact the pipe walls hots spots are identified. A similar pattern can be observed for the pebbles surface temperature distribution. As expected temperatures are lower close to the preferential channels. A detailed view of the pebbles shows how the heat transfer is lower where there are contacts with the pipe wall. The results show a good temperature distribution on the pebbles and a good heat extraction.

Current simulation example gives a valuable insight on the thermal hydraulic behaviour of the packed bed and can be used to optimize the coolant system. It also shows that the system can be properly cooled with the proposed layout.

4.3. Thermo-mechanical

The thermo-mechanical analysis is presented in three stages: load specification, thermal analysis, and mechanical analysis. The thermo-mechanical simulations were performed with the code Abaqus© 2018 using stationary thermal and mechanical analysis with sequential coupling.

4.3.1. Load specification

Main Blanket loads include thermal loads, internal pressure, inertial loads (gravity and seismic), EM loads. The thermo-mechanical model relies on a high uncertainty on the loads and operational conditions of STEP. In this sense, a dimensioning exercise of pebbles and pipes is done first. Then, a qualitative analysis of the structural concept is presented. Later, some

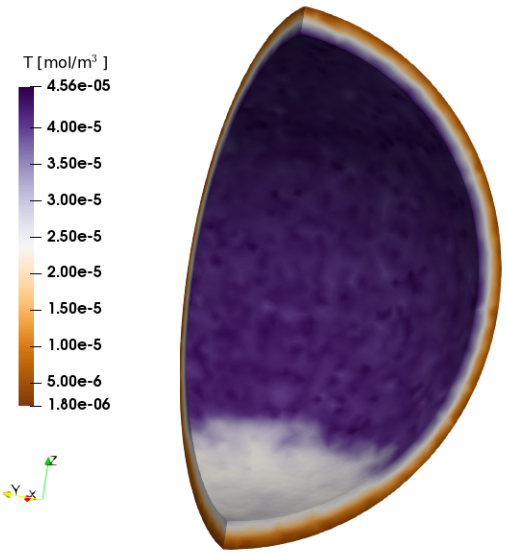

Figure 15: Q distribution in the FLiBe-Shell interface.

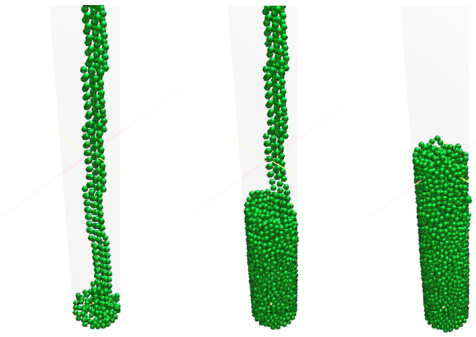

Figure 16: Detail of the mesh used for the thermal hydraulic analysis of the packed bed.

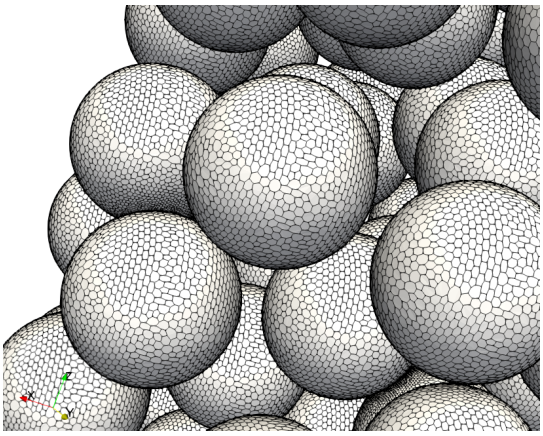

Figure 17: Detail of the mesh used for the thermal hydraulic analysis of the packed bed.

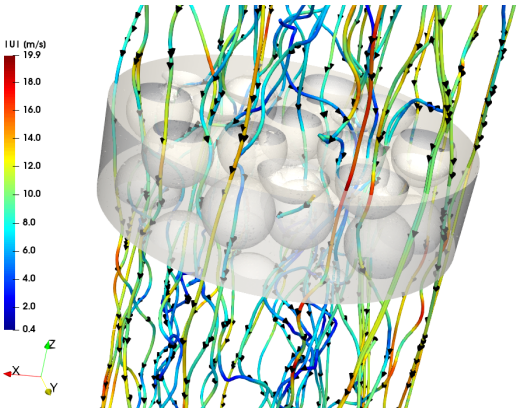

Figure 18: Detail of the packed bed velocity streamlines.

plausible load scenarios are postulated to see the effects on the material temperatures and stresses on the structural material, and to have an idea of design limits and main design challenges.

Thermal loads are caused by direct plasma radiation and neutronic heat deposition. It is assumed that direct plasma radiation does not affect the BB, as it is stopped by the First Wall. Thermal loads are applied in a thermal model of the Blanket to obtain a temperature field. The neutronic sources considered for the plasma are sketched in Fig. 21 and Tab. 6 (see e.g. [26], [27]).

Such temperatures are applied as thermal expansion loads to the mechanical problem (one-way coupling), and the material allowables decrease with temperature. Thermal expansion is fundamental for the dimensioning of the structural supports, which constraint the expansion generating stress. Thermal loads may cause compressions in the pipes, so thickness (slenderness) or side supports need to be dimensioned accordingly. Finally, the cooling of the BB shall be balanced to avoid thermal gradients causing local stress.

The generated heat inside structural material, breeder, and multiplier, needs to be extracted. The main heat exchange occurs inside the BU pipes, and it can be preliminarily considered that all the heat generated inside the pebbles is extracted by the N_2 flow. This holds true if the heat conduction (driven by the solid thermal contacts between jails) is low compared to the forced convection (driven by the coolant velocity and pressure). Then, the effective HTC at the BU wall of this pebble bed with nuclear heat generation is roughly the in-bed HTC of a passive bed. Passive pebble beds (without jails) are studied in [28], and some operational ranges expected are depicted in Tab. 7. Some heat extraction occurs also at the supports, with an assumed temperature of 100ºC.

Internal pressure shall be driving the thickness of the pipes in the layout (Sec. 3.6.2). The structural importance of internal pressure determines the applicability of, e.g., PED [29] and ESP/ESPN [30, 31], which are very demanding in terms of project supervision, 100% volumetric inspectability of pressure retaining welds, and need of periodic inspections.

Inertial loads (gravity and seismic) are dependent on the seismic behaviour of the placement of STEP. However, based on the experience in ITER, EM loads are generally more demanding.

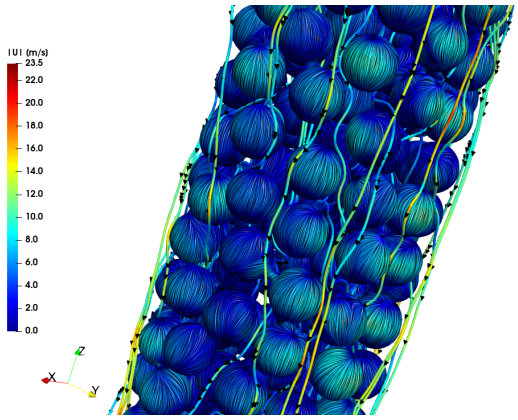

Figure 19: Packed bed velocity streamlines and Large Integral Convolution (LIC) on the pebbles surface.

Plasma	**Power** (eV/s)	**Description**
P-1	1.0e18	ITER-like plasma scenario
P-2	1.0e17	STEP-like plasma scenario

Table 6: Plasma scenarios.

EM loads arise as Lorentz forces produced by plasma disruptions, and Maxwell forces due to the ferromagnetic nature of the BB structural material. These EM loads are expected to dimension the blanket structures, especially the supports. Additionally, due to the topological features of slender pipe structures discussed in Sec. 3.6.2, EM forces need to be estimated and checked in the pre-conceptual phase. The EM loads are dependent on plasma disruptions, which is a characteristic of STEP. Based on previous work in ITER [32], the EM loads are approximated as a linear distribution of volumetric forces in space that creates reactions of about 400 kN in each of the 4 supports considered. Several scenarios are postulated: Moment-Y (torsion), Moment-X (bending), Double-Moment-Z (torsion), ... Moment-X (bending) is identified as the most critical scenario, with very similar results for topologies PC and HC.

4.3.2. Global thermal behaviour

The thermal behaviour of the load ranges in section 3.6.2 has been studied. The temperature distribution for P-1 and C-2 is shown in Fig. 22. In the NCEF proposed geometry, the multiplier experiences significant heating at the front area. However, the temperature is driven by the distance to the cooling (BU pipes), so a different pipe configuration can minimize this issue. Additionally, the highest temperature in the structural material is located at the front (top and bottom manifolds), falling in the High Temperature region of Eurofer 97 (above 450ºC). Some front sections of the BU pipes also fall in the Hight Temperature region, but the problem is closely related to the overheating of the multiplier.

The temperature profiles for different plasma and coolant configurations is analogous, and the quantitative changes in maximum values is reported in Table 8.

4.3.3. Global mechanical behaviour

The pipe thickness can be dimensioned based on internal pressure (primary load). The high temperature pipes are driven by their creep resistance. The pipe dimensioning must take into account that the creep allowable S_t shall be checked instead of the instantaneous allowable S_m (see RCC-MRx in [33]). Assuming an outer radius of the pipes of 56 mm, the different thickness depending on the temperature, the internal pressure an loads are shown in Table 9. Provisions shall be taken to minimize thermal stress, for instance enabling free thermal expansion in the axial direction of the pipes with an adequate design of the supports. Note that if the fatigue is not reduced by design, a significant drop in the allowable stress is expected.

The mechanical assessment is reported for the thermal loads with plasma P-1 and coolant C-2. The internal pressure has been taken as 8 MPa, which is very convenient for efficiency of the Brayton cycle if we use a single-loop plant [34].

It can be assumed that the creep-fatigue interaction criterion is valid for dimensioning the structure working in the HT range (front pipes, front manifold areas). Provisions against creep damage shall be taken for constant primary loads (gravity + pressure). Since the creep allowable S_t is strongly dependent on the creep-fatigue interactions, provisions against cyclic thermal loads shall be taken in the design, Sec. 3.6.2.

Additionally, thermal cyclic loads produce progressive deformation (Level A) for cyclic secondary loads (pressure + gravity + thermal), which involves higher loads but also higher allowable $3S_m$. However, for Eurofer 97 in the LT range, these are enveloped by the instantaneous secondary loads, which are limited by the more stringent IPFL (Levels A and C) with allowable S_e. The most demanding behaviour at the cold areas of the BB (support, rear manifold area, rear pipes) is shown for HC topology with plasma P-1 and cooling C-2, Fig. 24.

The thermal cyclic loads for the structure HC loaded with plasma P-1 and cooling C-2 is presented in Fig. 25, together with its potential for mitigation using a structural type PU. Remarkably, the most fatigued zones are not located at the front, mitigating creep-fatigue interactions in the HT areas: the fatigue at the front is driven by local gradients at thermal hotspots. Conversely, the loads at the cold areas and supports are significantly affected by the overall structural temperature, and the stiffness of the connections to the supporting structures. A detailed assessment of the supports needs to be carried out for more advanced design stages.

4.4. Manufacturability

Among liquid breeders, one of the most stable, safest and easy to manufacture is FLiBe. Note that FLiBe presents less difficulties when compared to PbLi, as the eutectic generation is difficult.

Taking advantage of the low melting temperature, FLiBe can be enclosed even in solid state, while breeding at reactor operation temperatures as a liquid. Available processes are focused on Styropor® coatings (see [35], namely, polymers with very low mechanical properties and melting point 240°C). Current process is readily available to produce hollow spheres

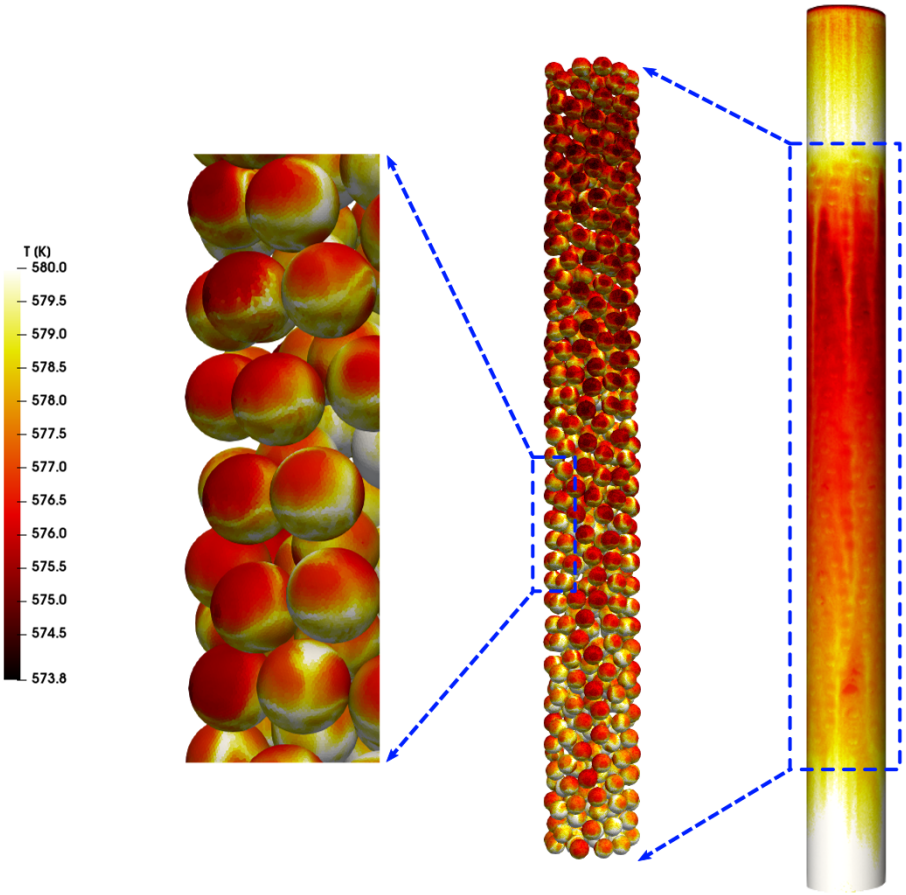

Figure 20: Temperature distribution in the packed bed.

with a small access (as a hole in the ceramic shell) where the breeder material (FLiBe) is inserted, then the hollow sphere is sealed. In this case, the mixture breeder-ceramic green material is avoided, but the sealing of the sphere might lead to similar problems. Note that alternative processes based on growing layers of ceramic on "frozen" pebbles of breeder could be extremely beneficial.

As has already discussed the preferred metallurgical alloy is Eurofer 97. The material can be cold worked to obtain seamless pipes in large batches, sheets, and wrought material for the manifolds; no difficulties are expected. The manifolds can be either manufactured by TIG, orbital welding and Electron Beam Welding (EBW) (Fig. 26) among others.

An important feature is the assembly of closure lids, enabling the breeder to be introduced at a late stage in the assembly; the heat treatment of the final lids can be done locally (without affecting the breeder). The multiplier and the reflector can be placed outside the pipes as packed bed (small pebbles or compressed powder). For structural finishing, a CFC plate can be fitted into the assembly.

4.5. Safety and waste management

The main aspect of a working breeding blanket is safety, so following must be enforced:

- All the blanket materials have to be chosen so that activation is reduced as much as possible.
- Use of non-toxic materials.
- Leakages of activated fluids shall be avoided.
- Prevent or mitigate accidents (e.g. LOCA).
- Easy waste segregation.

The breeding material contains Be, which is encapsulated in the pebbles. Note that the design is breeder-leakage resistant: if the liquid breeder leaks out a pebble, it will either flow to the lower manifold or solidify. To provision the former case, the manifold contains a lower plenum that allows leaked breeder to accumulate without having an impact on the blanket performance. In the later case, the FLiBe will either seal the pebble upon solidification or precipitate to the lower manifold. The low vapour pressure of FLiBe also prevents in-box LOCA.

The main issue working with N as coolant is not only its activation (see e.g. [14]), but also the $N^{14}(n,p)C^{14}$ nuclear reaction

Cooling	Pressure (MPa)	Flow velocity (m/s)	Flow temp. (ºC)	Film coefficient ($\frac{W}{m^2C}$)	Δp in 1 BU (Pa)
C-1	1	1	400	432	127
C-2	4	5	400	3708	1232
C-3	8	10	400	10432	3276

Table 7: Cooling scenarios for the BB. Film coefficient was obtained from [28] for pebble heat exchange, pressure drop for 1 BU was calculated from CFD model in Sec. 4.2.2.

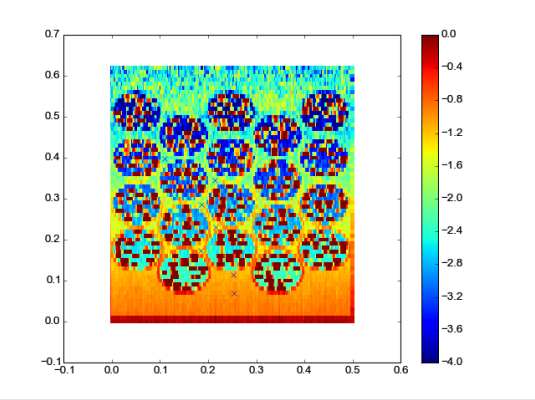

Figure 21: Nuclear heating of a section of NCEF ($log_{10}\frac{MW}{m^3}$) under plasma scenario P-1; scale in the fuel is limited for better detail in the structural material.

Plasma	Cooling	Multiplier (ºC)	Structure (ºC)
P-1	C-1	1751	677
P-1	C-2	1588	551
P-1	C-3	1571	534
P-2	C-1	535	427
P-2	C-2	518	415

Table 8: Thermal results: maximum temperatures for different plasma and cooling scenarios.

which has a significant cross-section for fast neutrons [36]. It can be assumed that radiocarbon will have to be removed from the system. Note that radiocarbon is also generated in nuclear water reactors [37] and in graphite reflectors, so the technology for removing it from the coolant streams is well-known.

Regarding the PbS multiplier, the nuclear reactions with sulphur generate radioactive isotopes with half lives below 90 day, like $S^{35}(n,\gamma)S^{34}$ with 87 days. Note that a common problem with Pb is that Po^{209} and Po^{210} and Bi radioactive isotopes are generated. However, using purified Pb for PbS should reduce the problem dramatically as discussed elsewhere [38]. Note also that as PbS does not generate gasses, in-box LOCA is not possible.

The use of WB as reflector may generate Q and He [39] due to the $B^{10}(n,\alpha)Li^7$ reaction. However, depending on the design the generation can be dramatically reduced as the neutron absorption probability rapidly decreases below 2.5MeV. If WC is used, He will also be generated along with Be^9 due to the $C^{12}(n,\alpha)Be^9$, but swelling is the only expected issue.

T (ºC)	P (MPa)	$th_{V=0}$ (mm)	$th_{V=0.2}$ (mm)
500	4	0.96	4.48
550	4	1.47	6.67
500	8	1.88	8.30
550	8	2.87	11.91

Table 9: : Selection of thickness for the BU pipes due to inner pressure: sensitivity analysis. The design shall enforce low fatigue usage factor ($\downarrow V$) through free axial thermal expansion or non-cycling loads to reach thickness below 5 mm.

The presented design uses a RAFM steel as structural material, which has enhanced radiation activation available material compared to the parent material ASTM P91, and can work with the selected blanket operating temperature window and mechanical loads.

Waste segregation has been accounted for in the design by the assembly sequence: the multiplier and the reflector can be removed by machining the assembly lids, then the pebbles can be extracted from the pipes and can be processed separately. Afterwards, the structural material is isolated from breeder and multiplier. Concerning the pebbles, as FLiBe will be solid once the blanket is removed from the reactor, cutting the jail and crushing the shell for processing should not be an issue.

5. Conclusions

The presented concept shows the possibility of manufacturing a blanket with conventional techniques at a reduced cost compared to other designs and a TBR>1.1. The design uses nitrogen to cool the blanket despite other coolants (e.g. He) are known to have a better performance, but they are either scarce or have large pumping requirements. Nitrogen can also be used in a direct power generation cycle and it not only cools down the structure, but it also removes Q from the breeder. This configuration allows a single pressure system, reducing the complexity of the blanket. As the coolant also carries Q, the N activation, which is less significant, poses no problem for the system. Note that by selecting a gas coolant instead of a liquid metal, water or a molten salt, the corrosion (among other phenomena) is no longer a problem.

The cooling scheme is simple from the performance and the manufacturing points of view: a series of vertical (poloidal) tubes, connected by a top and bottom manifold distribute the coolant from front (plasma side) to back. Therefore, the pressure requirements are limited to the pipes and the two manifolds.

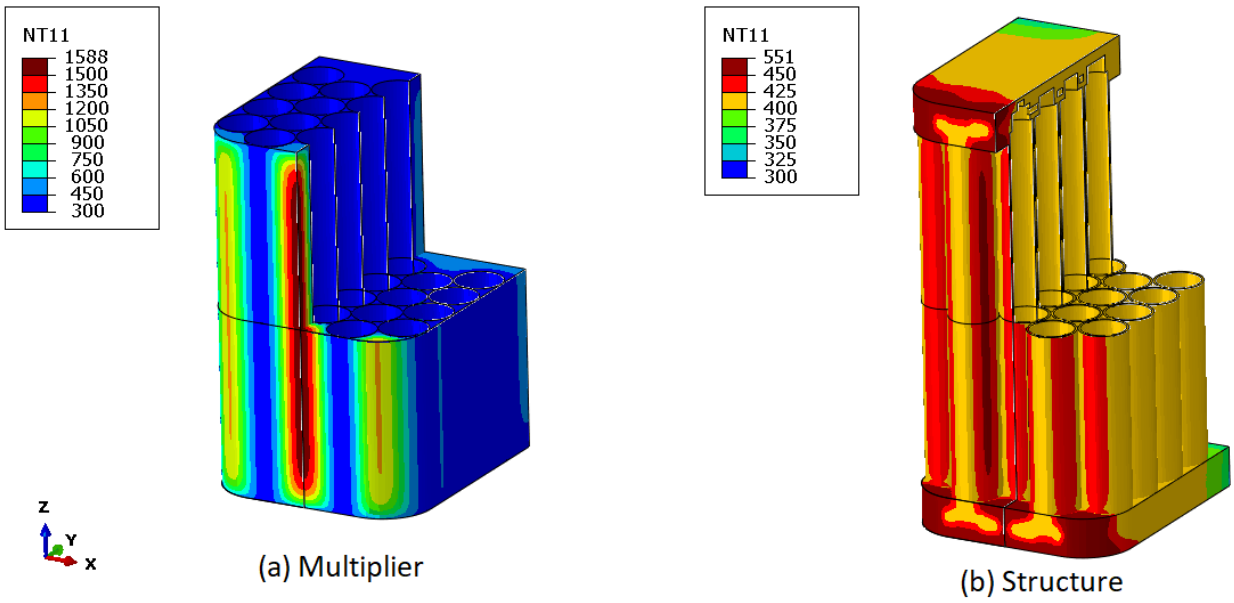

Figure 22: Temperatures on the multiplier (left) and the structure (right) for plasma P-1 and cooling C-2.

The breeder material has been tentatively selected to be FLiBe, which also contributes to the neutron multiplication. The working temperature of the blanket is mainly limited by the material working windows. The structural material, Eurofer 97, works between 300°C and 550°C. FLiBe eutectic 0.531 has a melting point of 363.5°C (with very high viscosity) which increases until 458.9°C for the 0.328 X-eutectic (with lower viscosity), which has a 2:1 LiF:BeF_2 composition. Therefore, the breeder will be liquid in operation, but can be solid during manufacturing. Note that Q extraction is dramatically improved by having the breeder material in liquid state.

Note that the breeder material generates He at a similar rate as Q, then an extraction method that prevents He pressure build up is necessary. The design encapsulates the breeder material in pebbles that allow the extraction of He and Q through a porous shell while keeping the breeder contained; two barriers are then present, the pebbles and the pipes.

The pebbles have been designed as a porous shell containing the FLiBe surrounded by a metallic jail. The jail prevents contact between porous media and helps the bed structural integrity. This design also ensures that any FLiBe leakage does not stop the blanket safe operation. Note that the design allows different breeder materials as they are contained in single pebbles.

An additional multiplier is necessary to achieve a TBR>1. In spite of a lower Pb content than other compounds, PbS was proposed because it is available in large quantities at a very low cost. The proposed structural topology enables the use of different multiplier materials filling the space among pipes.

A reflector was also considered at the back of the breeder zone. The neutronic simulations showed that the reflector was not necessary at this location, as it only works as shielding. In further design refinements, it could be used to maximize the neutron flux in the blanket by shielding the manifolds at the front and facing the pipes. The reflector can also be conceived as part of the multiplier packed bed.

The mechanical design is based on a topology of pebbles inside pipes, with upper and lower manifolds. These pipes are pressurized, and shall also withstand EM and thermal loads mainly. The selection of structural topology aims at alleviating thermal constraints to improve the thermal behaviour.

The thermo-mechanical analysis of these Eurofer 97 structures depends strongly on the blanket temperature (driven by the plasma and cooling operational conditions of the fusion plant), coolant pressure (driven by cooling), and the EM loads (driven by the plasma characteristics). A sweep of operational plasma, cooling, and EM conditions was made, reporting results presumably more conservative than the likely operational cases. The thermal results show a localized heating at the front areas of the BB, with several design corrections to be implemented, and manageable ”pessimistic” conditions: ITER plasma, 8 MPa, intermediate HTC. The mechanical results show creep problems at this hot area, but the creep-fatigue is less critical because thermal alternating stresses are expected mainly in the cold areas. Additionally, the loads at the cold areas and supports are significantly affected by the overall structural temperature, and the stiffness of the connections to the supporting structures. The proposed structural concept gives freedom to increase the degree of constraint up to a honeycomb structure to improve the EM behaviour.

The manufacturing of pebbles shall be based on ceramic coatings and hollow spheres (Hollomet). The readily available existing processes do not allow to create tight spheres grown on FLiBe material, then some research (with a sound baseline process) is required.

The manufacturing of the structure is feasible for Eurofer 97,

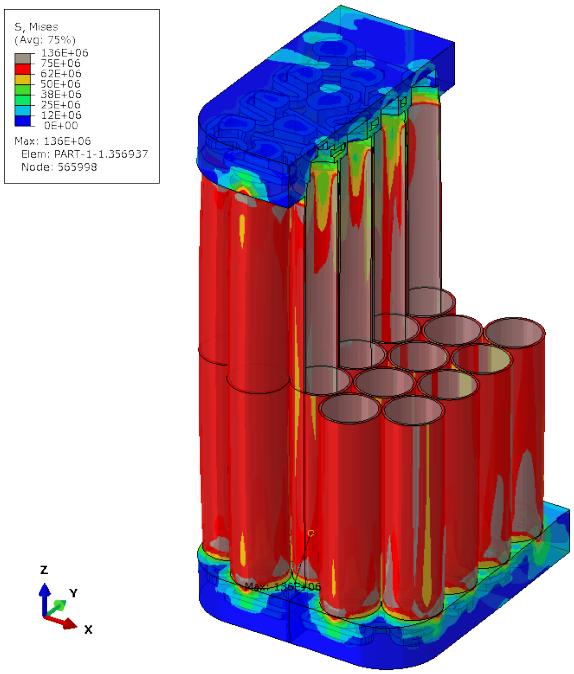

Figure 23: Mises stress [Pa] for HC structure with monotonic primary loads: plasma P-1, cooling C-2, internal pressure 8 [MPa], gravity, EM Moment-X (bending). This load case dimensions the hot areas of the BB (front manifold areas, front pipes) to be provisioned against creep and creep/fatigue (allowable S_t).

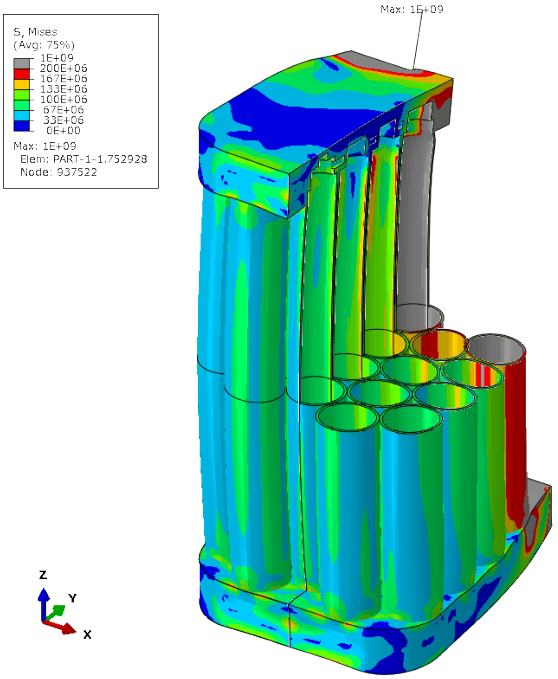

Figure 24: Mises stress [Pa] for HC structure with monotonic primary and secondary loads: plasma P-1, cooling C-2, internal pressure 8 [MPa], gravity, EM Moment-X (bending). This load case dimensions the cold areas of the BB (support, rear manifold areas, rear pipes) to be provisioned against IPFL (allowable S_e).

based on state-of-the-art technologies. Such technologies can make use of EBW or orbital welding. No stoppers were found for the current design stage.

6. Acknowlegments

The authors would like to thank UKAEA and Nuclear AMRC for their collaboration and for providing all necessary data to carry out the presented work.

References

[1] G. Aiello, J. Aubert, L. Forest, J.-C. Jaboulay, A. L. Puma, L. Boccaccini, Design of the helium cooled lithium lead breeding blanket in CEA: from TBM to DEMO, Nuclear Fusion 57 (2017) 046022.

[2] K. Schleisiek, H. U. Borgstedt, F. Dammel, H. Feuerstein, A. Fiege, U. Fischer, H. Gerhardt, H. Glasbrenner, T. Jordan, K. Kleefeldt, W. Kramer, P. Norajitra, G. Reimann, H. Reiser, G. Schmitz, H. Schnauder, R. Stieglitz, Kernforschungszentrum Karlsruhe (1994).

[3] L. Boccaccini, N. Bekris, Y. Chen, U. Fischer, S. Gordeev, S. Hermsmeyer, E. Hutter, K. Kleefeldt, S. Malang, K. Schleisiek, I. Schmuck, H. Schnauder, H. Tsige-Tamirat, Design description and performance analyses of the european hcpb test blanket system in iter feat, Fusion Engineering and Design 61-62 (2002) 339 – 344.

[4] R. A. Causey, R. A. Karnesky, C. San Marchi, Tritium barriers and tritium diffusion in fusion reactors, Comprehensive Nuclear Materials 4 (2012) 511–549.

[5] J. Fradera, S. Cuesta-López, The effect of a micro bubble dispersed gas phase on hydrogen isotope transport in liquid metals under nuclear irradiation, Fusion Engineering and Design 88 (2013).

[6] J. Fradera, S. Cuesta-López, Nucleation, growth and transport modelling of helium bubbles under nuclear irradiation in lead-lithium with the self-consistent nucleation theory and surface tension corrections, Fusion Engineering and Design 88 (2013).

[7] J. Fradera, S. Cuesta-López, Impact of nuclear irradiation on helium bubble nucleation at interfaces in liquid metals coupled to permeation through stainless steels, Fusion Engineering and Design 89 (2014).

[8] F. Hernández, P. Pereslavtsev, First principles review of options for tritium breeder and neutron multiplier materials for breeding blankets in fusion reactors, Fusion Engineering and Design 137 (2018) 243–256.

[9] R. Romatoski, L. Hu, Fluoride salt coolant properties for nuclear reactor applications: A review, Annals of Nuclear Energy 109 (2017) 635–647.

[10] B. Sorbom, J. Ball, T. Palmer, F. Mangiarotti, J. Sierchio, P. Bonoli, C. Kasten, D. Sutherland, H. Barnard, C. Haakonsen, J. Goh, C. Sung, D. Whyte, ARC: A compact, high-field, fusion nuclear science facility and demonstration power plant with demountable magnets, Fusion Engineering and Design 100 (2015) 378–405.

[11] C. Wong, S. Malang, M. E. Sawan, I. Sviatoslavsky, E. Mogahed, S. Smolentsev, S. Majumdar, B. Merrill, R. Mattas, M. Friend, J. Bolin, S. Sharafat, Molten salt self-cooled solid first wall and blanket design based on advanced ferritic steel, Fusion Engineering and Design - FUSION ENG DES 72 (2004) 245–275.

[12] E. Morse, Fusion Technology, Springer International Publishing, 2018, pp. 413–479.

[13] P. Masset, R. A. Guidotti, Thermal activated (thermal) battery technology: Part II. Molten salt electrolytes, Journal of Power Sources 164 (2007) 397–414. URL: https://www.sciencedirect.com/science/article/abs/pii/S0378775306022592. doi:10.1016/J.JPOWSOUR.2006.10.080.

[14] E. Ibe, H. Karasawa, M. Nagase, M. Endo, S. Uchida, M. Utamura, Chemistry of radioactive nitrogen in BWR primary system, Journal of Nuclear Science and Technology 26 (1989) 844–851.

[15] J. H. Owston, Reactivity analysis of a direct nuclear heated gas turbine with nitrogen coolants, Nuclear Engineering and Design 355 (2019) 110355.

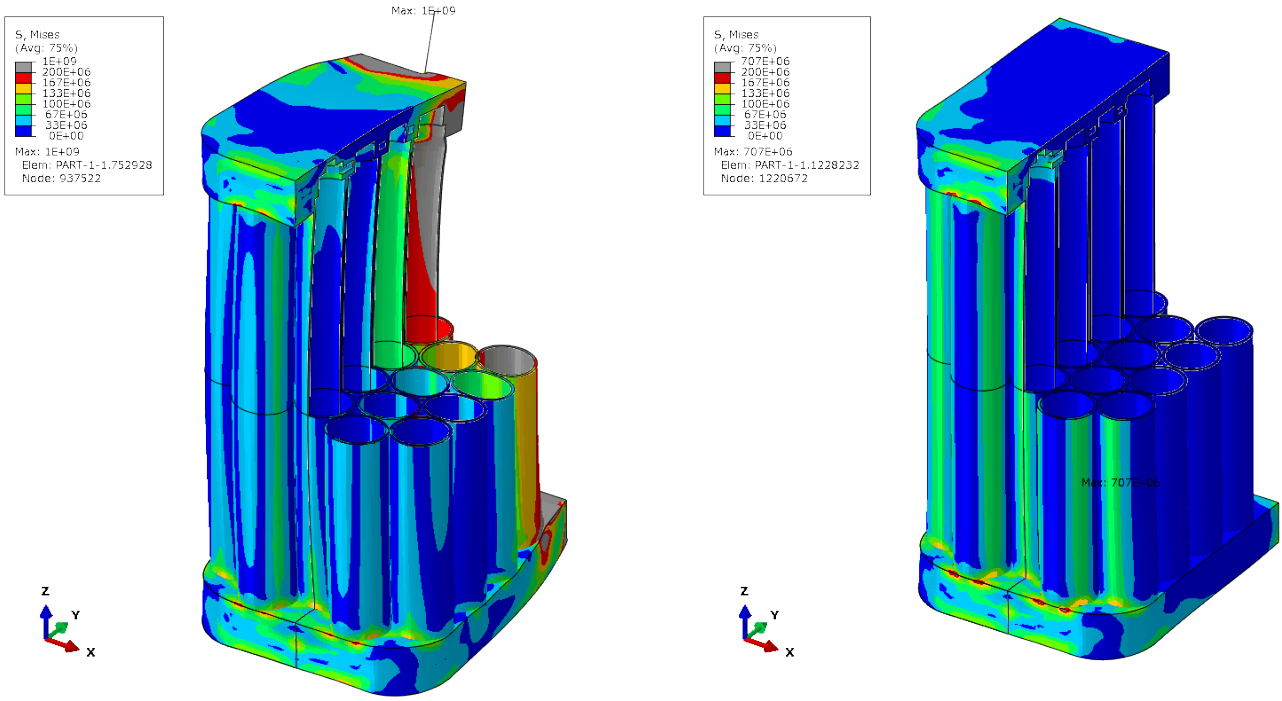

(a) HC structure

(b) PU structure

Figure 25: Mises stress [Pa] for cyclic loads in highly-constrained HC (a) and slightly-constrained PU (b) structures: plasma P-1, cooling C-2.

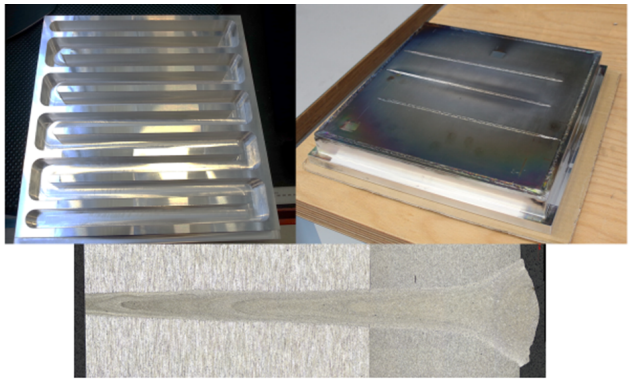

Figure 26: Nuclear AMRC Aluminium cooling block and E-Beam penetration profile on the same part.

[16] E. Rabaglino, Helium and Tritium in Neutron-irradiated Beryllium, Forschungszentrum Karlsruhe (2004).

[17] S. A. Humphry-Baker, G. D. Smith, Shielding materials in the compact spherical tokamak, Philosophical Transactions of the Royal Society A: Mathematical, Physical and Engineering Sciences 377 (2019).

[18] RCC-MRx, Demande de modification / Modification request DMRx number: 10-115 A3. Gen et A3.19AS eurofer dated: 28.06.2010 (????).

[19] J. Aktaa, M. Walter, G. Angella, E. Perelli Cippo, Creep-fatigue design rules for cyclic softening steels, International Journal of Fatigue 118 (2019) 98 – 103. URL: http://www.sciencedirect.com/science/article/pii/S0142112318303566. doi:https://doi.org/10.1016/j.ijfatigue.2018.08.008.

[20] K. Zhang, J. Aktaa, Ratcheting and fatigue behavior of eurofer97 at high temperature, part 2: modeling, Fusion Engineering and Design 152 (2020) 111426. URL: http://www.sciencedirect.com/science/article/pii/S0920379619309226. doi:https://doi.org/10.1016/j.fusengdes.2019.111426.

[21] J. Aktaa, Y. Carin, J. Vallory, Non-linear assessment of critical failure modes in the first wall of the european tbm, Fusion Engineering and Design 128 (2018) 223 – 230. URL: http://www.sciencedirect.com/science/article/pii/S092037961730947X. doi:https://doi.org/10.1016/j.fusengdes.2017.11.032.

[22] J. Shimwell, S. Lilley, L. Morgan, L. Packer, M. Kovari, S. Zheng, J. McMillan, Reducing beryllium content in mixed bed solid-type breeder blankets, Fusion Engineering and Design 109-111 (2016) 1564 – 1568. doi:https://doi.org/10.1016/j.fusengdes.2015.11.021, proceedings of the 12th International Symposium on Fusion Nuclear Technology-12 (ISFNT-12).

[23] T. Eade, M. Garcia, R. Garcia, F. Ogando, P. Pereslavtsev, J. Sanz, G. Stankunas, A. Travleev, Activation and decay heat analysis of the european demo blanket concepts, Fusion Engineering and Design 124 (2017) 1241 – 1245.

[24] M. Sohal, M. Ebner, P. Sabharwall, P. Sharpe, Engineering Database of Liquid Salt Thermophysical and Thermochemical Properties, Idaho Natl. Lab. Idaho Falls CrossRef (2010).

[25] S. Flaischlen, G. D. Wehinger, Synthetic packed-bed generation for cfd simulations: Blender vs. star-ccm+, 2019.

[26] i. Štancar, M. Gorelenkova, S. Conroy, J. Eriksson, J. Buchanan, L. Snoj, Generation of a plasma neutron source for monte carlo neutron transport calculations in the tokamak jet, Fusion Engineering and Design 136 (2018). doi:10.1016/j.fusengdes.2018.04.065.

[27] A. V. Zhirkin, B. V. Kuteev, Three-dimensional model of DEMO-FNS facility considering neutronics and radiation shield problems, Heliyon 5 (2019). URL: https://doi.org/10.1016/j.heliyon.2019.e01630. doi:10.1016/j.heliyon.2019.e01630.

[28] E. Achenbach, Heat and flow characteristics of packed beds, Experimental Thermal and Fluid Science 10 (1995) 17 – 27. URL: http://www.sciencedirect.com/science/article/pii/089417779400077L. doi:https://doi.org/10.1016/0894-1777(94)00077-L.

[29] PED 2014/68/EU, Directive of the European Parliament and of the council of 15 May 2014 on the harmonisation of the laws of the Member States relating to the making available on the market of pressure equipment, ????

[30] ESP Decree, Decree 99-1046 of 13/12/1999 on Pressure Equipment EN, ????

[31] ESPN Order, French Order 30 December 2015 for Nuclear Pressure

Equipment, ????

[32] R. Muñoz, F. J. Calvo, S. Sádaba, A. M. Gil, J. Rodríguez, J. Vallory, M. Zmitko, Y. Poitevin, Analysis of test blanket module attachments under electromagnetic loads by using a dynamic amplification factor envelope, Fusion Engineering and Design 136 (2018) 1247–1251. URL: https://www.sciencedirect.com/science/article/abs/pii/S0920379618304046. doi:10.1016/J.FUSENGDES.2018.04.110.

[33] RCC-MRx, Design and Construction Rules for Mechanical Components of Nuclear Installations, ????

[34] J. Park, J. Yoon, J. Eoh, H. Kim, M. Kim, Optimization and sensitivity analysis of the nitrogen Brayton cycle as a power conversion system for a sodium-cooled fast reactor, Nuclear Engineering and Design 340 (2018) 325–334. doi:10.1016/j.nucengdes.2018.09.037.

[35] Hollomet, Hollomet - Hollow spheres, 2020.

[36] M. S. Yim, F. Caron, Life cycle and management of carbon-14 from nuclear power generation, Progress in Nuclear Energy 48 (2006) 2–36.

[37] W. J. Davis, CARBON-14 PRODUCTION IN NUCLEAR REACTORS, Technical Report TM-12, 1977.

[38] G. L. Khorasanov, A. P. Ivanov, A. I. Blokhin, Polonium issue in fast reactor lead coolants and one of the ways of its solution, International Conference on Nuclear Engineering, Proceedings, ICONE 2 (2002) 711–717.

[39] G. Hollenberg, B. Mastel, Helium bubbles in irradiated boron carbide (1979).